Supporting Information

Biotinylation of Silicon and Nickel Surfaces and Detection of Streptavidin as Biosensor

Hirokazu Seto,[†] Chie Yamashita,[†] Seiji Kamba,[‡] Takashi Kondo,[‡] Makoto Hasegawa,[§] Mitsuhiro Matsuno,[§] Yuichi Ogawa,[] Yu Hoshino,[†] Yoshiko Miura[†*]

[†] Graduate School of Engineering, Kyushu University, 744 Motooka, Nishi-ku, Fukuoka 819-0395, Japan.

[‡] Murata Manufacturing Company, 1-10-1 Higashikotari, Nagaokakyo 617-8555, Japan.

[§] Graduate School of Bioscience, Nagahama Institute of Bio-Science and Technology, 1266 Tamura, Nagahama, Shiga 526-0829, Japan

[] Graduate School of Agriculture, Kyoto University, Kitashirakawaoiwake-cho, Sakyo-ku, Kyoto 606-8502, Japan.

* Corresponding author. Yoshiko Miura
Tel: +81-92-802-2749
Fax: +81-92-802-2769
E-mail: miuray@chem-eng.kyushu-u.ac.jp

1. Physical properties of the 100 THz-operating Ni mesh

The 100 THz-operating Ni mesh was used as the substrate of the MMD sensor. The original Ni mesh had lattice-shaped morphology with square holes of 1.8 μm, grid intervals of 2.6 μm, and effective surface area of 67 mm^2 (Figure S1).

The transmission properties of the MMD sensors are determined by their geometric parameters. Incident electromagnetic waves to the MMD excite surface plasmon polariton (SPP)-like surface wave derived from diffraction anomaly through periodic openings. The electric field is enhanced and localized near the openings with excitation of surface wave. Because of this physical phenomenon, the extraordinary transmission, which was higher than opening ratio of the MMD, was observed in the range from 80 to110 THz in the transmittance spectrum of the original Ni mesh. In addition, a dip structure was observed at 95 THz. The transmission dip appears due to the focusing incident beam. The frequency of the dip structure was overlapped with the absorption band of water. The measurement taken at the dry conditions was therefore required to allow for the operation at around 100 THz. The MMD sensing in the mid-infrared range, however, led to a high sensitivity.

The sensing method relies on a change of the transmittance shift to the lower frequency when the analytes is applied on the mesh surface. Since the resonant frequencies of these transmission peak and dip strongly depend on the refractive index of the MMD surface, the extremely small amount of the analytes can be determined by the shift magnitude of the transmission dip.

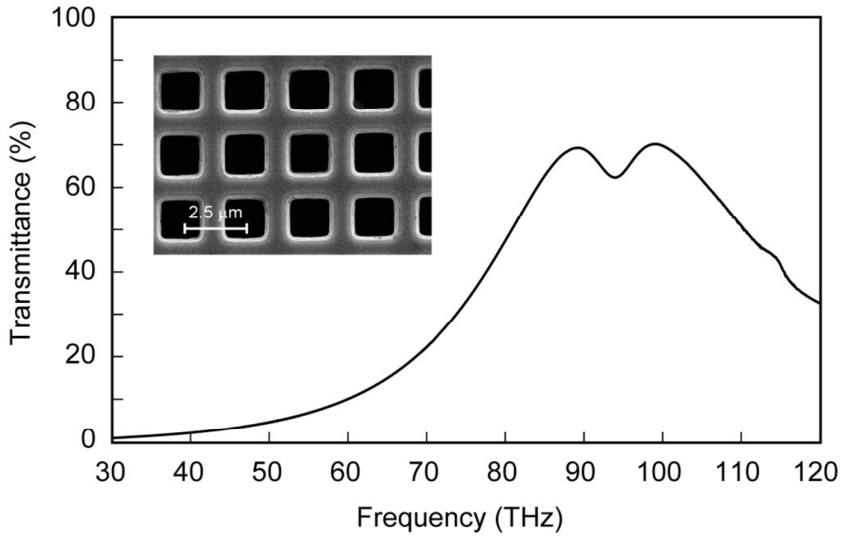

Figure S1. Scanning electron microscopic image and transmittance IR spectrum of the unmodified Ni mesh.

2. Confirmation of amination and maleimidation on Si and Ni surfaces

The occurrence of the amine, maleimide, and biotin groups on the Si and Ni surfaces was confirmed by XPS analysis, as shown in Figures S2 and S3. The main atoms detected on the surface were carbon (1s), nitrogen (1s), oxygen (1s), silicon (2p), and nickel (2p). The sulfur atoms of the biotin reagent could not be detected because of below the detection limits of the spectrometer. Peaks corresponding to the silicon and metal oxides were observed in the O(1s), Si(2p), and Ni(2p) XPS spectra of the unmodified Si and Ni surfaces; SiO_x (531.9 eV and 102.5 eV), NiO (529.7 eV and 854.1 eV). The treatment involving the aqueous mixture of hydrogen peroxide and ammonia led to the formation of an oxidized layer, and ultimately facilitated the silane coupling reaction for the amination of the Si and Ni surfaces. The intensities in the C(1s) and N(1s) spectra sequentially increased with processing surface modification. In contrast, the intensities in the Si(2p) and Ni(2p) spectra were reduced, indicating that X-ray irradiation onto the substrate surface was interfered by the amination, maleimidation, and biotinylation. In the O(1s) spectra of the Ni surfaces, two peak tops were observed. The peak at the lower binding energy corresponded to the component of the metal oxide, whose intensity was significantly reduced following the biotinylation of the Ni surface. In spite of this reduction, the Si(2p) and Ni(2p) spectra were clearly visible, estimating that the biotin layers formed on the surfaces were thin, because the resolution depth of the XPS was within 10 nm.

Adsorption of streptavidin (10^{-1} g L^{-1}) onto the biotinylated Si and Ni surfaces was also confirmed by XPS analysis (Figures S2 and S3). The intensities in the C(1s) and N(1s) spectra of the streptavidin-adsorbed surfaces were stronger than that of the biotinylated surfaces, especially the peak corresponding to the C=O of peptide bond in protein (287.7 eV) was predominant.

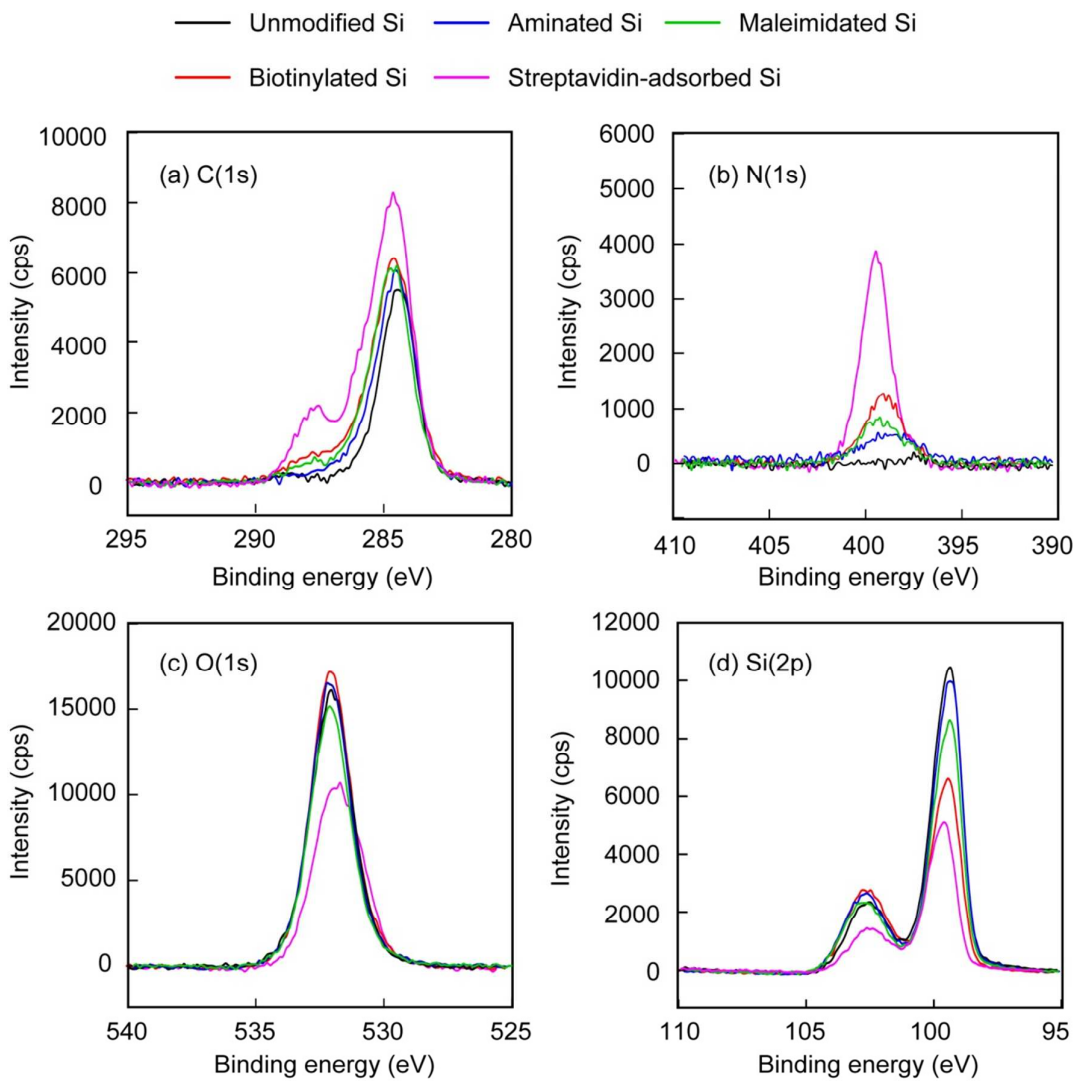

Figure S2. X-ray photoelectron spectra of the unmodified, aminated, maleimidated, and biotinylated Si wafers; (a) C(1s), (b) N(1s), (c) O(1s), and (d) Si(2p).

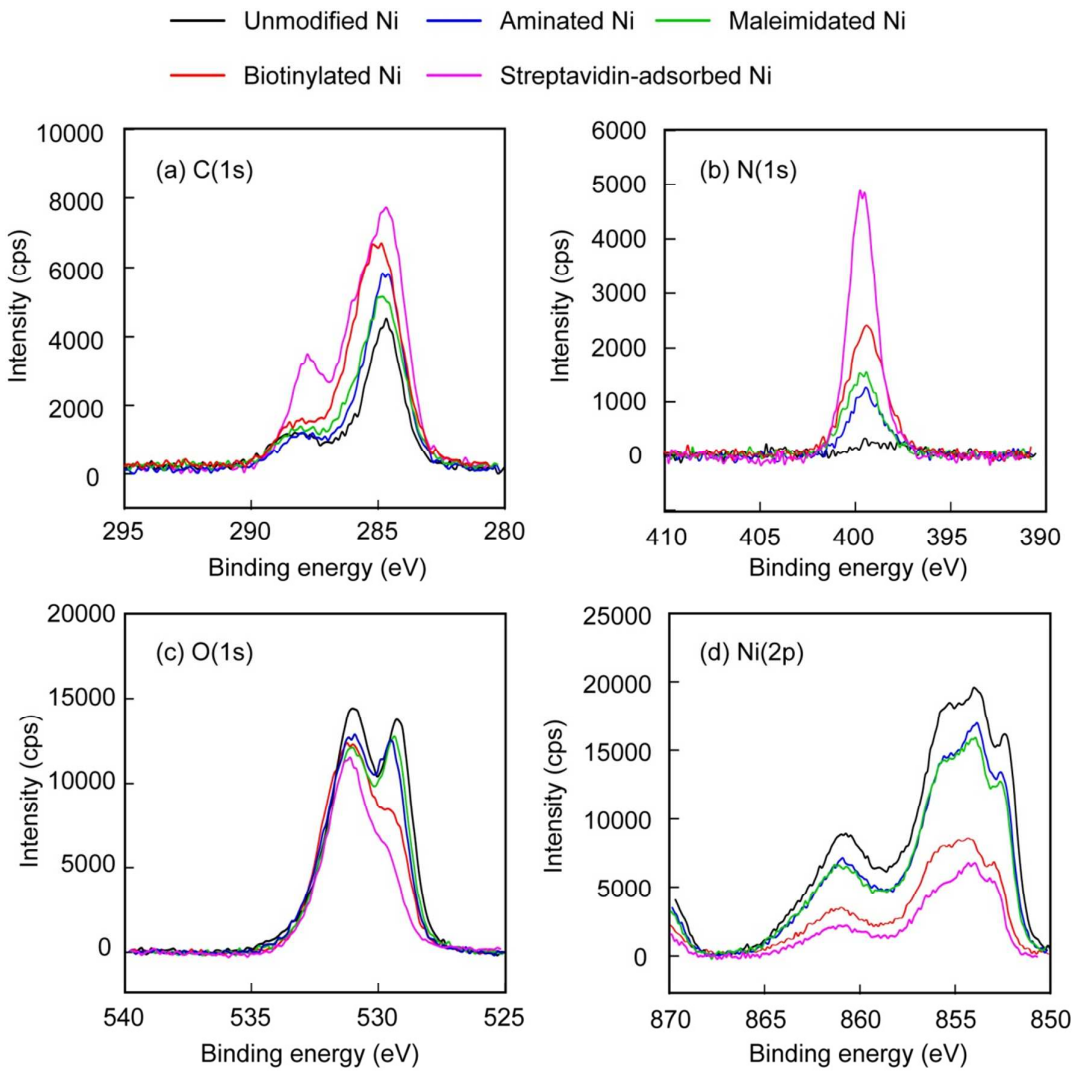

Figure S3. X-ray photoelectron spectra of the unmodified, aminated, maleimidated, and biotinylated Ni meshes; (a) C(1s), (b) N(1s), (c) O(1s), and (d) Si(2p).

3. Comparison of the molar ratio obtained from the QCM determination with the value from the XPS determination

The molar ratio on the Si surface, which was estimated from the QCM determination, was compared with the value estimated from the XPS determination. The differences in the atomic percentage from the previous step (i.e. ΔC/Si, ΔN/Si, and ΔO/Si), which were estimated from the XPS determination, are shown in Table S1. The carbon/nitrogen ratios on the aminated, maleimidated, and biotinylated surfaces were 4.6, 6.0, and 5.9, respectively. These values were close to the theoretical carbon/nitrogen ratios. Following immobilization, the APTMS, SMP, and HS-$(CH_2)_{11}$-NH-C(O)-biotin possess 3, 7, and 21 carbons per molecule, respectively (Figure S4). Therefore, the molar ratio of the amine, maleimide, and biotin, estimated from the ΔC/Si values of the XPS determination, was 11:7:1. When the QCM measurements were performed at dry conditions, the Δm values of the amine, maleimide, and biotin were determined to be 11.4, 2.8, and 0.32 nmol cm^{-2}, respectively (i.e. a molar ratio of 36:9:1). This molar ratio was similar to the ratio found in the XPS results.

The amount of streptavidin adsorbed was also quantified from the XPS determination. The carbon/nitrogen ratio on the streptavidin-adsorbed surface was also in agreement with the theoretically determined value. The chemical formula of the streptavidin subunit is $C_{720}H_{1107}N_{205}O_{241}$. Therefore, the molar ratio between the immobilized biotin and streptavidin was 10:1. When the QCM measurements were performed using the biotinylated SiO_2 oscillator with 1.93×10^{14} molecules cm^{-2}, the Δm_{max} of streptavidin was determined to be 4.04×10^{12} molecules cm^{-2}. Therefore, the molar ratio between the immobilized biotin and streptavidin was 48:1, which was comparable with the value estimated from the XPS results.

Table S1 ΔC/Si, ΔN/Si, and ΔO/Si Values, Carbon/Nitrogen Ratios, and Theoretical Carbon/Nitrogen Ratios on Aminated, Maleimidated, Biotinylated, and Streptavidin-Adsorbed Surfaces.

	ΔC/Si	ΔN/Si	ΔO/Si	C/N	Theoretical C/N
Aminated	0.18	0.04	<0.00	4.6	3.0
Maleimidated	0.28	0.05	0.05	6.0	7.0
Biotinylated	0.12	0.02	0.21	5.9	7.0
SAv-adsorbed	1.62	0.48	0.12	3.4	3.5

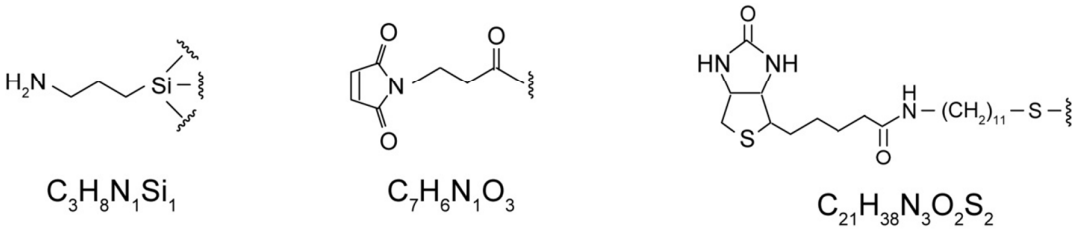

Figure S4 Chemical structures and formulae of APTMS, SMP, and HS-$(CH_2)_{11}$-NH-C(O)-biotin remained after immobilization.

4. Frequency changes during streptavidin adsorption on the biotinylated SiO_2-oscillator of the QCM cell

The amount of streptavidin adsorbed on the biotinylated surface was determined by QCM measurements (AFFINIXQ4, Initium Inc., Tokyo, Japan). The time course of frequency changes during streptavidin adsorption on the biotinylated SiO_2-oscillator of the QCM cell is shown in Figure S5. The frequency of the QCM with the biotinylated oscillator was initially stabilized at the dry conditions. When the QCM cells were filled with a phosphate buffer solution, the frequency of the QCM with the biotinylated oscillator was significantly reduced, and then eventually reached a steady state. Following the injection of streptavidin solutions into the frequency-stabilized QCM cells, the frequency was negatively changed. The frequency values were equilibrated within 30 min, indicating that streptavidin was rapidly bound to the biotin on the surface. After being washed sequentially with the buffer solution and water, and then dryed in a dryer at 40°C, the QCM was measured at the dry conditions. After 2 h, the frequency became constant. The values of ΔF_{air} were estimated from the frequencies at the dry conditions before and after the adsorption of streptavidin.

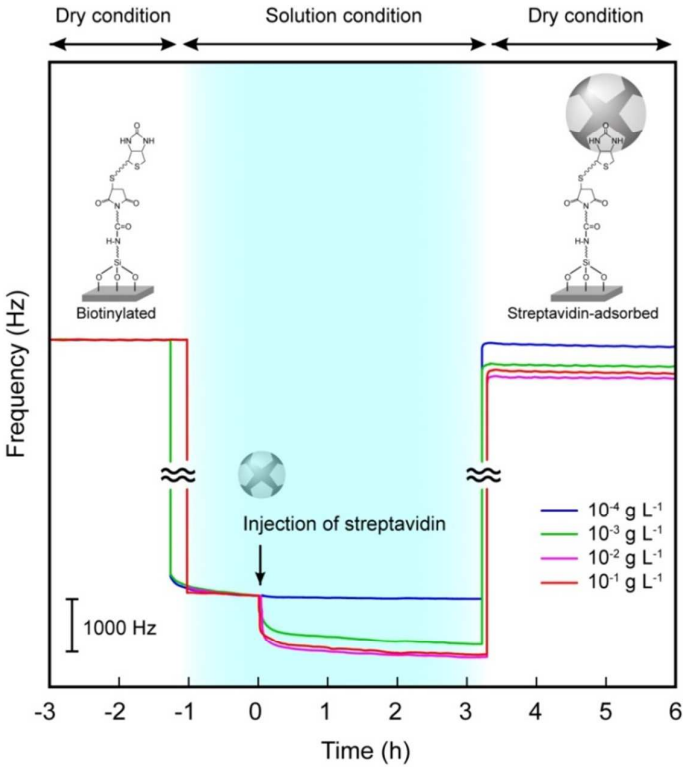

Figure S5. Time course of the frequency changes during streptavidin adsorption on the biotinylated SiO_2-oscillator of the quartz crystal microbalance cell at dry and solution conditions

5. Transmittance spectra of the 100 THz-operating Ni mesh

Changes in the refractive indices on the surface of the metal mesh lead to spectral shifts in the transmittance, when a sample is attached to the surface. The magnitudes of the shifts in the dipped peaks in the transmittance spectra of the Ni mesh adsorbed with streptavidin were dependent on the concentration of streptavidin used (Figure S6). The transmittance spectrum of each Ni mesh was rapidly obtained within 2 min. The measurement time of MMD sensing for $-\Delta f$ was significantly shorter than that of QCM for $-\Delta F_{air}$.

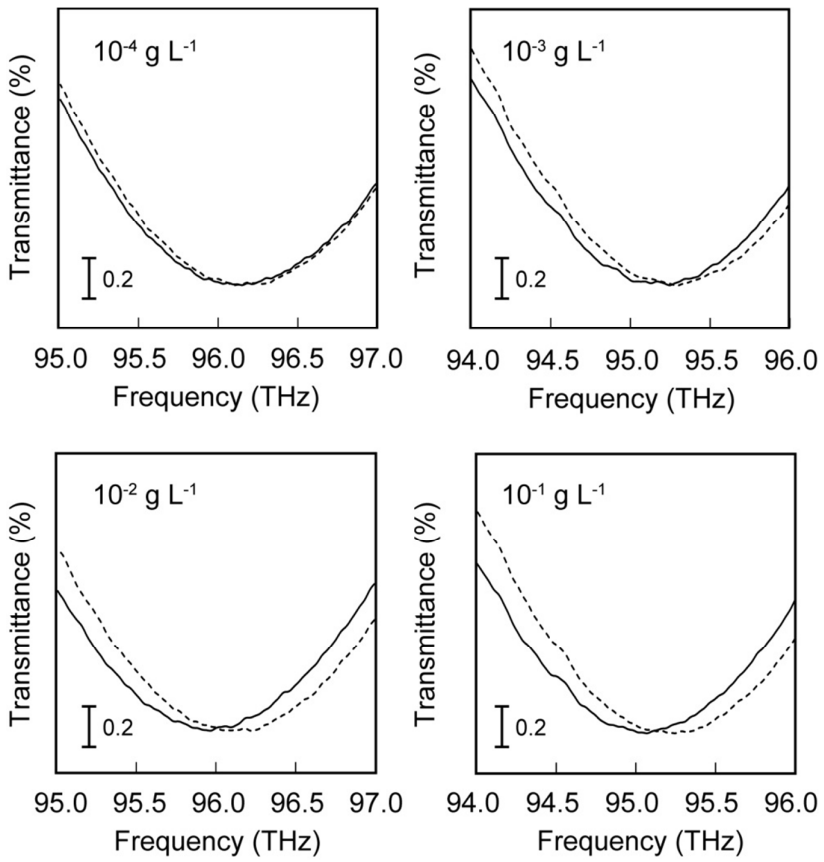

Figure S6. Transmittance infrared spectra of the Ni mesh before and after the adsorption of streptavidin; dashed lines: biotinylated Ni meshes, and solid lines: streptavidin-adsorbed Ni meshes.

6. Amount of streptavidin adsorbed on biotinylated Ni mesh, determined by electrophoresis

The Ni meshes, adsorbed with streptavidin at 10^{-1} g/L, were immersed in the eluent at 98°C for 5 min. The eluent was prepared by adding DL-dithiothreitol (0.1 mol/L), bromophenol blue (50 mg/L), sodium dodecyl sulfate (20 g/L), and glycerol (10 wt%) to a Tris-HCl buffer solution (6 mmol/L, pH: 6.8). The eluted streptavidin was cast onto the poly(acrylamide) gel, and the electrophoresis experiments were then carried out for 1 h. The fractions of streptavidin on the gel were visualized using staining reagent such as SYPRO red. The surface of the gel was scanned using a fluorescent scanner (Figure S7-a). The concentration of eluted streptavidin was estimated from the total gray value of the electrophoretic band. The total gray values were obtained using ImageJ software. A calibration curve of the total gray value was prepared using standard solutions of streptavidin at a variety of different concentrations (Figure S7-b). The amount of streptavidin eluted was estimated to be 170 ng cm^{-2}.

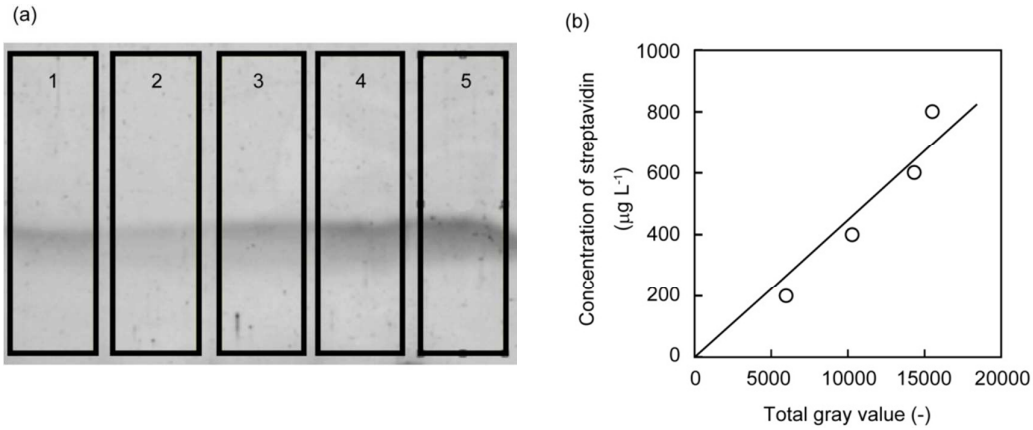

Figure S7. Determination of streptavidin concentration using electrophoresis with poly(acrylamide) gel. (a) Picture of poly(acrylamide) gel fractionated with streptavidin. Column No. 1: streptavidin eluted from biotinylated Ni mesh, No. 2: streptavidin standard with 200 μg L^{-1}, No. 3: streptavidin standard with 400 μg L^{-1}, No. 4: streptavidin standard with 600 μg L^{-1}, and No. 5: streptavidin standard with 800 μg L^{-1}. (b) Calibration curve between the total gray value and the streptavidin concentration.

7. Adsorption of biotin conjugate on streptavidin-immobilized glass slide

The binding of the biotin conjugate to streptavidin adsorbed on the biotinylated surface, i.e. biotin-streptavidin-biotin sandwich method (Figure S8), was evaluated using a fluorescent microarray. The biotinylated glass slide was immersed in streptavidin solution (100 mg L^{-1}), and then incubated for 3 h. The resulting streptavidin-immobilized glass slide was then washed and dried. A variety of different concentrations of biotin-4-fluorescein (FITC-biotin, AnaSpec, Inc., Fremont, CA, USA) in a phosphate buffer solution (pH: 7.4, 20 μL) were spotted onto the unmodified, biotinylated, and streptavidin-immobilized glass slides. The glass slides were incubated in the absence of light for 3 h and washed with water. The microspots on the glass slides were scanned using a microarray scanner (FLA-8000, Fujifilm Corporation, Tokyo, Japan) at 532 nm. The average gray values on the glass slides were obtained using the ImageJ software (National Institutes of Health, Bethesda, MD, USA).

The fluorescent images and gray values of microarray spots adsorbed with FITC-biotin are shown in Figure S9. On the unmodified glass slide, FITC-biotin was not adsorbed across the entire range of the fluorophore concentration because of the hydrophilicity of the surface. The fluorescent spots of the FITC-biotin were observed on the biotinylated glass slide above 1×10^{-6} mol L^{-1}, in which the FITC-biotin was nonspecifically bound to biotin on the surface by hydrophobic interactions. Meanwhile, the FITC-biotin was detected on the streptavidin-immobilized glass slide using a lower concentration of the fluorophore, (i.e. 5×

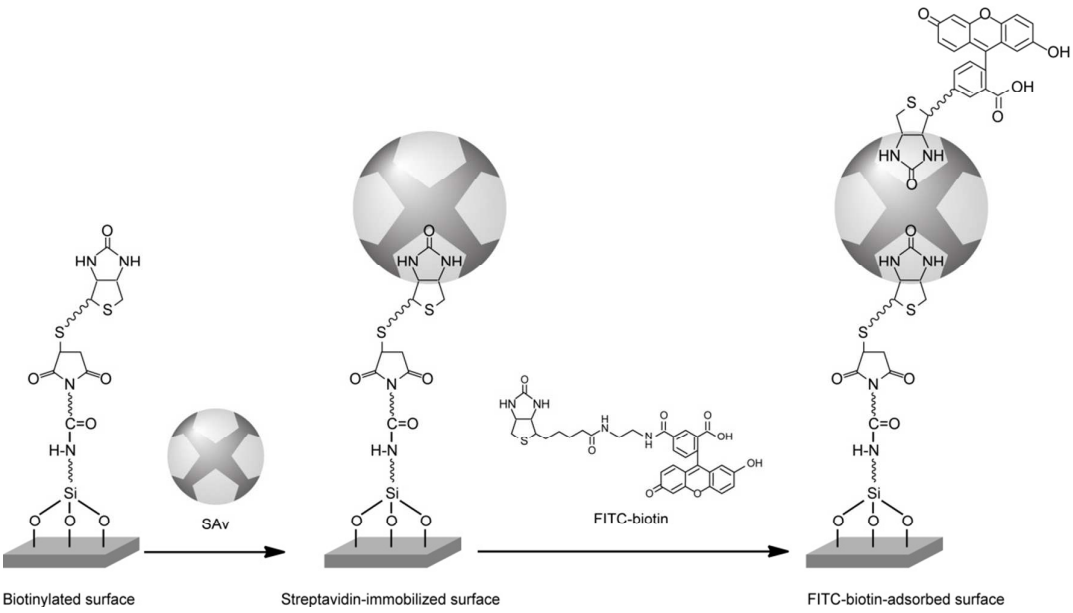

Figure S8. Adsorption of the biotin conjugate on the streptavidin-immobilized surface via biotinylation.

10^{-8} mol L^{-1}). These results suggested that the high recognition ability of the immobilized streptavidin against biotin remained. Biotin conjugates, such as the biotinylated protein and DNA, can be immobilized using biotin-streptavidin-biotin sandwich method.

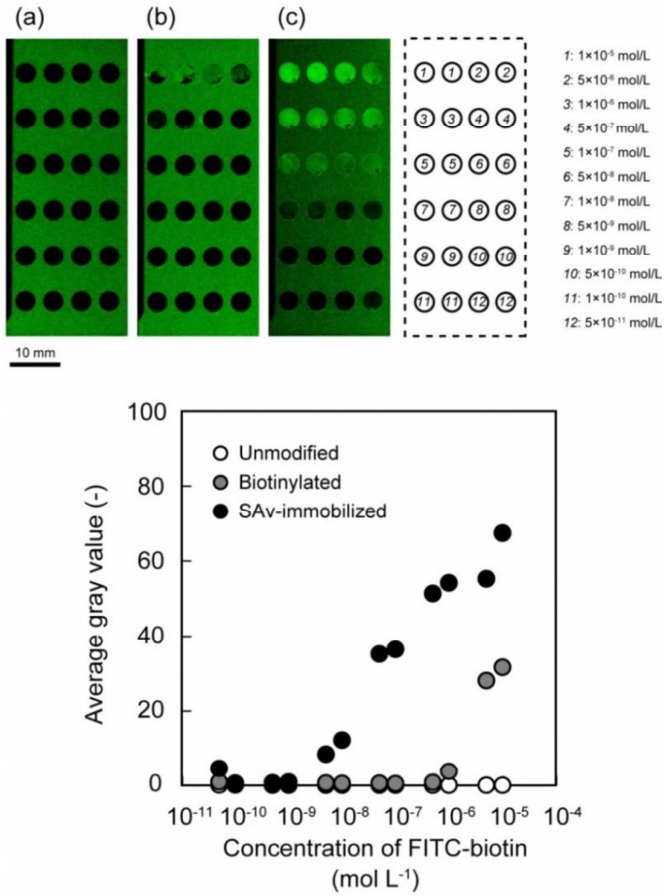

Figure S9. Average gray values on the (a) unmodified, (b) biotinylated, and (c) streptavidin-immobilized glass slides *versus* the concentration of FITC-biotin.